Coupling of Voltage Sensing to Channel Opening Reflects Intrasubunit Interactions in Kv Channels

Alain J. Labro, Adam L. Raes, and Dirk J. Snyders

Laboratory for Molecular Biophysics, Physiology, and Pharmacology, Department of Biomedical Sciences, University of Antwerp, Antwerp 2610, Belgium

ABSTRACT Voltage-gated K^+ channels play a central role in the modulation of excitability. In these channels, the voltage-dependent movement of the voltage sensor (primarily S4) is coupled to the (S6) gate that opens the permeation pathway. Because of the tetrameric structure, such coupling could occur within each subunit or between adjacent subunits. To discriminate between these possibilities, we analyzed various combinations of a S4 mutation (R401N) and a S6 mutation (P511G) in hKv1.5, incorporated into tandem constructs to constrain subunit stoichiometry. R401N shifted the voltage dependence of activation to negative potentials while P511G did the opposite. When both mutations were introduced in the same α-subunit of the tandem, the positive shift of P511G was compensated by the negative shift of R401N. With each mutation in a separate subunit of a tandem, this compensation did not occur. This suggests that for Kv channels, the coupling between voltage sensing and gating reflects primarily an intrasubunit interaction.

KEY WORDS: hKv1.5 • gating • S4 segment • S6 gate • dimers

INTRODUCTION

Voltage-gated K^+ channels (Kv channels) respond to changes in the electric field across the cell membrane by opening or closing the ion-conducting pore. They are composed of four individual α-subunits each containing six membrane-spanning helices (S1–S6) and a pore loop between S5 and S6. The S4 segment makes up the main part of the channel's voltage sensor that moves and/or reorients in response to a change in the membrane potential (for review see Bezanilla, 2000). This repositioning triggers the opening (or closing) of the cytoplasmic activation gate, which is considered to be located in the lower part of S6 (del Camino and Yellen, 2001). The crystal structures of the bacterial K^+ channels KcsA, MthK, KirBac, and KvAP suggest that the pore forming regions S5–P–S6 of each subunit are assembled in a tetrameric configuration with intra- and intersubunit interactions (Doyle et al., 1998; Jiang et al., 2002, 2003; Kuo et al., 2003). Based on these structures, a gating model has been proposed in which the movement of the voltage sensor (regions S2–S4), proposed to be directly attached to the S5 helix, might open the pore by pulling S5 away from the central pore axis and causing the S6 helix to follow. In this model, S5 and S6 move together as one unit, suggesting an intrasubunit interaction between voltage sensing and gate opening (Jiang et al., 2003). However, this mechanism could be different in eukaryotic Kv channels because the structure of the voltage sensor may differ from the KvAP's voltage sensor "paddle" (Gandhi et al., 2003; Laine et al., 2003; Lee et al., 2003; Ahern and Horn, 2004; Starace and Bezanilla, 2004) and because of the presence of a functionally important PXP motif in the S6 domain that is absent in KvAP (Labro et al., 2003). Furthermore, other channel segments might be involved in gating since several studies have provided evidence for interactions between the S4–S5 linker and residues in the COOH-terminal part of S6 in HERG, HCN, and *Shaker* (Lu et al., 2002; Tristani-Firouzi et al., 2002; Ding and Horn, 2003; Decher et al., 2004). Since subunit cooperativity is a recurrent feature in the various kinetic models of channel gating (Tytgat and Hess, 1992; Zagotta et al., 1994; Schoppa and Sigworth, 1998), the question arises whether the mechanism that couples voltage sensing to gate opening reflects an interaction between neighboring subunits or whether it occurs within the same subunit. This is an important question because the answer will determine whether this coupling mechanism acts largely independently within each subunit or whether it reflects a highly cooperative interaction between neighboring subunits. To discriminate between both hypotheses, we analyzed an S4 mutation in combination with an S6 mutation in human Kv1.5 tandem constructs to control the subunit stoichiometry (Liman et al., 1992).

MATERIALS AND METHODS

Molecular Biology

hKv1.5 was expressed using a pBK-CMV expression vector and mutations were introduced as described previously (Labro et al.,

Correspondence to Dirk J. Snyders: dirk.snyders@ua.ac.be

J. Gen. Physiol. © The Rockefeller University Press • 0022-1295/2005/01/71/10 $8.00
Volume 125 January 2005 71–80
http://www.jgp.org/cgi/doi/10.1085/jgp.200409194

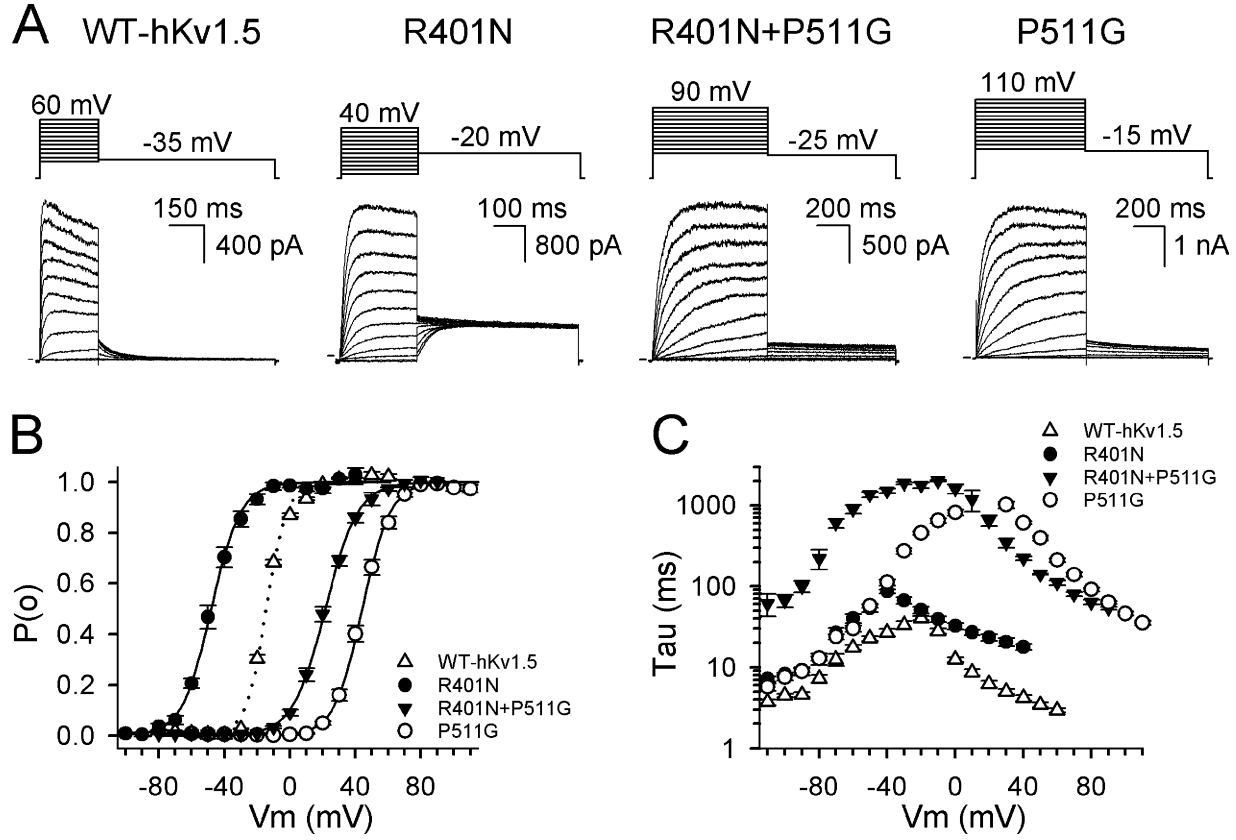

FIGURE 1. Biophysical properties of channels containing WT-hKv1.5, R401N, P511G, or R401N+P511G monomers. (A) Raw current traces elicited by the voltage protocol shown on top. From left to right, the current recordings of WT-hKv1.5, the mutant R401N, the double mutant R401N+P511G, and the mutant P511G. The horizontal bar on the left indicates the zero current level. Notice the difference in the threshold of activation. (B) Voltage dependence of activation. R401N (circles) shifted the activation curve toward negative values while P511G (open circles) shifted it toward positive potentials, compared with WT-hKv1.5 (dotted line). Note that the double mutant R401N+P511G (inverted triangles) had an activation curve that was shifted toward WT values compared with P511G. (C) Activation and deactivation kinetics. R401N had time constants that were slightly slower than WT (open triangles). In contrast, P511G displayed marked slowing of activation and deactivation. The double mutant R401N+P511G had activation time constants similar to those of P511G but deactivated extremely slow (clearly slower than R401N or P511G).

2003). Tandem constructs were obtained by creating a first and a second hKv1.5/pBK-CMV vector, each representing the first and the second subunit of the tandem. In the first vector, the stop codon was removed (replaced by a serine codon) together with the introduction of an Xba1 restriction site. In the second vector, an Xba1 site was inserted three nucleotides upstream of the start ATG. Tandem constructs were subsequently created by cutting the hKv1.5 sequence out of the first vector with Hind3/Xba1 and ligate it in the second vector that had been digested with Hind3/Xba1. This yielded a tandem with two complete hKv1.5 sequences linked together with a three amino acid–long linker. The mutations R401N or P511G or double mutation R401N+P511G were introduced separately in the first or second vector before creating the tandems. Note that the hKv1.5 numbering used here refers to the original numbering of Tamkun et al. (1991) and used in our subsequent papers; in the revised numbering (accession no. P22460), R401 is R403 and P511 is P513.

Electrophysiology

Ltk$^-$ cells were cultured and transfected (1 μg cDNA) as described previously (Labro et al., 2003). Current recordings were made with an Axopatch-200B amplifier (Axon Instruments) in the whole cell configuration at room temperature; current recordings were low pass filtered and sampled with a Digidata-1200A data acquisition system (Axon Instruments). Command voltages and data storage were controlled with pClamp8 software (Axon Instruments). Patch pipettes were pulled from 1.2-mm quick-fill borosilicate glass capillaries (World Precision Instruments) with a P-2000 puller (Sutter Instruments) and heat polished. The cells were perfused continuously with a bath solution containing (in mM) NaCl 130, KCl 4, $CaCl_2$ 1.8, $MgCl_2$ 1, HEPES 10, glucose 10, adjusted to pH 7.35 with NaOH. The pipettes were filled with intracellular solution containing (in mM) KCl 110, K_4BAPTA 5, K_2ATP 5, $MgCl_2$ 1, HEPES 10, and adjusted to pH 7.2 using KOH. Experiments were excluded from analysis if the voltage errors originating from the series resistance exceeded 5 mV.

The holding potential was −80 mV in most experiments, but set to −90 mV for mutants containing the R401N mutation. The interpulse interval was at least 15 s, but was increased up to 45 s as needed for some mutants to prevent accumulation of slow inactivation. Voltage protocols (voltage range and step duration) were adjusted based upon the different biophysical properties of mutant channels. Activation and deactivation time constants were determined with a single or double exponential function; the goodness of the fit was judged by inspection of the residuals.

TABLE I

Biophysical Parameters for Voltage Dependence of Activation

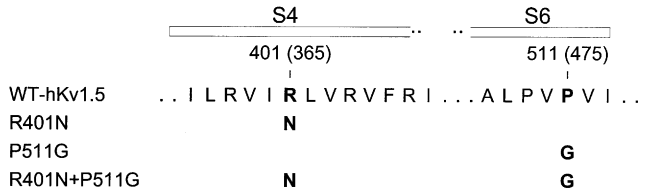

		$V_{1/2}$	k	ΔG0	*n*
		mV	*mV*	*kcal/mol*	
Monomeric			5.8 ± 0.2	−1.35 ± 0.11	9
WT-hKv1.5		−14.3 ± 1.0	9.3 ± 0.9	−2.81 ± 0.29	5
R401N		−47.9 ± 1.7	8.6 ± 0.2	2.79 ± 0.09	10
P511G		44.2 ± 1.2	10.0 ± 0.4	1.18 ± 0.08	5
R401N+P511G		21.6 ± 1.2			
Tandem constructs					
1st	*2nd*				
WT	WT	−6.5 ± 1.2	6.3 ± 0.2	−0.56 ± 0.11	12
R401N	R401N	−46.2 ± 0.6	9.9 ± 0.4	−2.55 ± 0.11	4
R401N	WT	−17.9 ± 1.6	7.7 ± 0.2	−1.27 ± 0.12	9
WT	R401N	−15.6 ± 1.5	8.4 ± 0.3	−1.01 ± 0.10	7
P511G	P511G	32.0 ± 1.0	9.2 ± 0.4	1.90 ± 0.11	7
P511G	WT	26.2 ± 0.9	13.6 ± 0.3	1.05 ± 0.08	8
WT	P511G	35.8 ± 0.4	11.9 ± 0.4	1.64 ± 0.06	6
R401N+P511G	R401N+P511G	12.7 ± 1.6	9.0 ± 0.4	0.77 ± 0.10	8
R401N+P511G	WT	10.0 ± 1.3	9.2 ± 0.3	0.59 ± 0.08	12
WT	R401N+P511G	13.0 ± 2.0	10.8 ± 0.6	0.66 ± 0.07	7
P511G	R401N	24.1 ± 0.8	13.1 ± 0.5	1.01 ± 0.07	6
R401N	P511G	31.8 ± 3.0	11.5 ± 0.5	1.51 ± 0.16	7

Top section, partial sequences of the S4 and S6 segments of WT-hKv1.5. The S4, the S6, and the double mutations are named according to their substitutions (indicated in bold). The residue numbering on top is for hKv1.5, with the *Shaker* numbering in parentheses. Main section, voltage dependence of activation of WT and mutant channels formed by monomeric or tandem subunits, as indicated. The configuration of WT and mutant subunit within a tandem construct is represented as *1st* and *2nd* subunit (starting from the NH_2 terminus). The midpoint of activation ($V_{1/2}$), slope factor (k), and ΔG_0 for the voltage dependence of activation were derived as described in MATERIALS AND METHODS. The results are expressed as mean ± SEM and *n* the number of cells. For raw current traces of dimers and tandem constructs see Figs. S2 and S3 (http://www.jgp.org/cgi/content/full/jgp.200409194/DC1).

Activation curves were fitted with a Boltzmann equation: $y = 1/(1 + \exp[-(E - V_{1/2})/k])$, with E the applied voltage, $V_{1/2}$ the midpoint potential, and k the slope factor. 1/k corresponds to zF/RT with z the equivalent charge, and F, R, and T have their usual meaning. The Gibbs free energy of activation at 0 mV (ΔG_0) was calculated by $\Delta G_0 = 0.2389zFV_{1/2}$, with the factor 0.2389 to express the values in cal/mol (Li-Smerin et al., 2000). Results are expressed as mean ± SEM.

Online Supplemental Material

The online supplemental material (Figs. S1, S2, and S3) is available at http://www.jgp.org/cgi/content/full/jgp.200409194/DC1. Fig. S1 shows current traces and properties of channels originating from either a cotransfection of WT and P511G subunits or from the tandem construct 1:WT_2:P511G. It demonstrates that the biophysical properties of channels originating from a cotransfection are clearly different from those of channels resulting from the tandem construct. In addition, it further highlights that both subunits of the tandem construct are integrated in the tetramer. Figs. S2 and S3 show the raw current recordings of all dimers and tandem constructs used.

RESULTS

Channel activation is thought to occur in a succession of conformational states that include the movement or reorientation of the voltage sensor and the opening of the channel gate. It has been suggested that the lower part of S6 forms the cytoplasmic activation gate while S4 has been considered to be the main part of the voltage-sensing domain. Therefore we selected in hKv1.5, a *Shaker*-type K^+ channel, one mutation in S4 and another in S6 that both altered the energetics of activa-

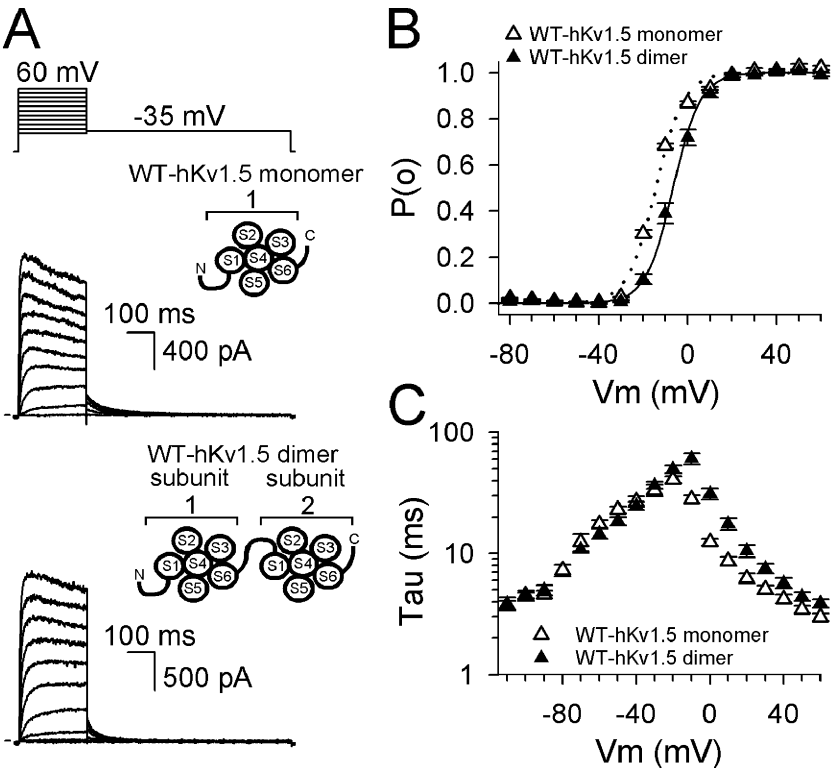

FIGURE 2. Biophysical properties of channels containing WT-hKv1.5 monomers or dimers. (A) Current traces of WT-hKv1.5 monomers and WT-hKv1.5 dimers. The voltage protocol is represented above the currents of channels formed form WT-hKv1.5 monomers or WT-hKv1.5 dimers, as indicated by the cartoon representation of a WT monomer and tandem construct as an inset. The monomer is a single α-subunit containing S1–S6. The tandem construct contains two α-subunits (1 and 2) with the COOH terminus of the first subunit ("1") linked to the NH_2 terminus of the second subunit ("2"). This 1 and 2 numbering is used throughout to designate the configuration of the different tandem constructs. In this and subsequent legends, dimer or monomer are shorthand for channels formed upon expression of dimers or monomers, respectively. (B) The voltage dependence of activation of WT-hKv1.5 monomer (open triangles) and dimer (filled triangles). The activation curve of the dimer was slightly shifted compared with that of the monomer. (C) Kinetics of activation and deactivation. The time constants of channels formed both from monomers ($n = 9$) and dimers ($n = 12$) were similar; note the semilogarithmic scale.

tion. These mutations were chosen on the basis of their location as well as their functional effects.

In the S6 segment, we used a glycine substitution of the second proline of the highly conserved P*X*P motif (Table I). This mutation (P511G) shifted the voltage dependence of activation by 60 mV toward positive potentials (Fig. 1, A and B; Table I), and slowed the kinetics of activation and deactivation ~10-fold compared with WT-hKv1.5 (Fig. 1 C) (Labro et al., 2003). The mutation in S4 (R401N) neutralized the second positive charge of the S4 segment and caused a hyperpolarizing shift of ~30 mV in the voltage dependence of activation (Fig. 1, A and B; Table I), similar to the effects of the corresponding R365N mutation in *Shaker* (Miller and Aldrich, 1996). The activation and deactivation time constants were slightly slower compared with WT-hKv1.5 (Fig. 1 C).

When both mutations were combined in the same subunit (R401N+P511G), the positive shift (P511G) was partially compensated by the negative shift (R401N), and the midpoint was shifted back toward WT values (Fig. 1, A and B; Table I). However, the compensation did not occur for the time constants. To express these shifts in midpoints as differences in the free energy between the closed and the open state, we calculated ΔG_0 (at 0 mV) for each mutant as described in experimental procedures. Consistent with the shifts of the activation curves, both mutations altered the ΔG_0 compared with WT (Table I) and the combination of both mutations (double mutant R401N+P511G) had a compensatory effect on the ΔG_0. According to the KvAP crystal structure (Jiang et al., 2003) and the latest *Shaker* channel models (Durell et al., 2004; Shrivastava et al., 2004), both residues R401 and P511 are most likely separated in space and their compensatory effect should thus not be due to close packing effects.

To discriminate between an inter- or intrasubunit interaction, it was necessary to control the stoichiometry of subunits in the tetrameric channel. Therefore, tandem subunits were constructed with predetermined locations of the S4 and the S6 mutations. The WT-hKv1.5 dimer had a voltage dependence of activation that was only slightly shifted (~8 mV) toward positive potentials, compared with channels derived from WT-hKv1.5 monomers (Fig. 2; Table I). The activation and deactivation time constants of both were comparable (Fig. 2 C). The biophysical properties of channels containing the R401N dimer were not significantly different from those containing the corresponding monomer (Fig. 3; Table I). For the P511G mutation the voltage dependence of activation of the dimer was shifted 12 mV toward negative potentials compared with the monomer (Fig. 3; Table I). The activation and deactivation time constants followed this shift (Fig. 3 B). The voltage dependence of the double mutant R401N+P511G dimer (Fig. 3; Table I) was similar to the monomer as it was shifted back toward WT values (Fig. 3 A). The activation and deactivation time constants of the R401N+P511G dimer compared well to those of the monomer (Fig. 1 C; Fig. 3 B), with slowed deactivation kinetics.

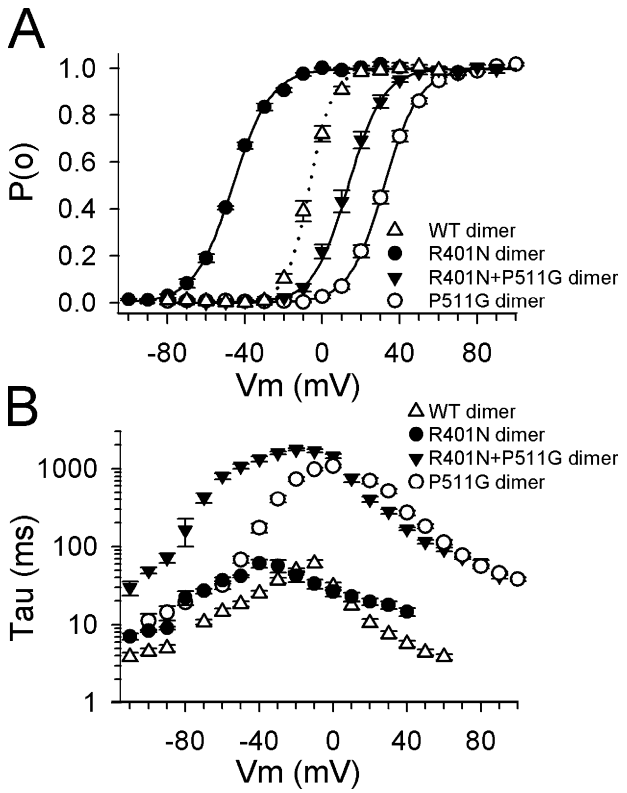

FIGURE 3. Comparison of WT, R401N, P511G, and R401N+P511G dimers. (A) Voltage dependence of activation. The activation curve of the R401N dimer (circles) was similar to that of the R401N monomer. The midpoints of the P511G dimer (open circles) and the R401N+P511G dimer (inverted triangles) were slightly shifted toward negative potentials compared with P511G and R401N+P511G monomers. Compared with the WT-hKv1.5 dimer (dotted line), the R401N and P511G dimer were still shifted toward negative and positive potentials, respectively. The double mutant R401N+P511G dimer had an activation curve that was shifted toward WT values compared with the P511G dimer. (B) Time constants of all dimers compared well with their corresponding monomers.

These results showed that the functional properties of channels composed of WT, R401N, P511G, or R401N+P511G monomers or dimers were similar. Therefore, the use of dimer constructs had minimal effects on gating. It has been suggested that only one of the subunits in a tandem construct may be incorporated in the functional tetrameric channel protein (McCormack et al., 1992). To exclude this possibility, we created tandem constructs that contained one mutant (R401N or P511G) subunit and one WT subunit in either the configuration *mutant–WT* or *WT–mutant*. If only a single subunit of the tandem would be included in the tetramer, we would expect clear functional differences between these two opposite configurations (*mutant–WT* and *WT–mutant*). The tandem with an R401N mutation in the first subunit and WT as second subunit (i.e., a 1:R401N_2:WT configuration) had properties that were indistinguishable from those of the opposite configuration (1:WT_2:R401N), but both were clearly different from the R401N dimer (Fig. 4 A; Table I). Both tandems had a midpoint of activation that was only 10 mV more negative than that of a WT-hKv1.5 dimer (Fig. 4 A; Table I). Furthermore, the time constants of activation and deactivation of these tandems compared more to those of the R401N dimer than those of the WT dimer, taking into consideration the shifts in voltage dependence of activation (Fig. 4 B). The tandems with a 1:WT_2:P511G and a 1:P511G_2:WT configuration (Fig. 4 C, top) had a positive midpoint potential similar to the P511G dimer and markedly different from WT (Fig. 4 C). In contrast to the R401N/WT tandems, the kinetics of the channels expressed from either the 1:WT_2:P511G or the 1:P511G_2:WT tandem were best fitted with a double exponential function in which the slow component compared well to the P511G gating, as expected if the slowly gating P511G subunit forms part of the tetramer. To confirm further the integration of both subunits of a dimer in a channel, the properties of the 1:WT_2:P511G tandem were compared with those of a cotransfection of WT and P511G subunits (Fig. S1, available at http://www.jgp.org/cgi/content/full/jgp.200409194/DC1). In the case of the cotransfection, a mixed population of channels with binomially distributed ratios of subunits is expected. The biophysical properties derived from the currents of this mixed population were clearly different from the ones obtained with the tandem construct, strengthening the idea that both subunits of the dimer were integrated in a functional channel. All together, these results with oriented tandems and cotransfections strongly indicate that both subunits of the tandem constructs were assembled in a tetrameric channel. The raw current traces for all constructs in Fig. 4 are shown in Fig. S2 (available at http://www.jgp.org/cgi/content/full/jgp.200409194/DC1).

The results above indicated that the R401N mutation could compensate for the positive shift of the P511G mutation in a monomeric (Fig. 1) and tandem configuration (Fig. 3). Furthermore, in tandems with one WT and one mutant subunit, channel opening was found to be determined largely by the gating machinery with the most positive voltage dependence of activation, which was WT for the WT/R401N cases (Fig. 4 A), and P511G for the WT/P511G combinations (Fig. 4 C). Thus, combining a single S4 and S6 mutation in all possible positional combinations in tandem subunits should allow us to determine if the gating machinery that couples voltage sensitivity to gate opening is an inter- or intrasubunit interaction. To investigate the hypothesis of an intrasubunit interaction, tandem constructs with one WT and one double mutant (R401N+P511G) subunit were created (Fig. 5 A, top). The reference construct for these experiments was the

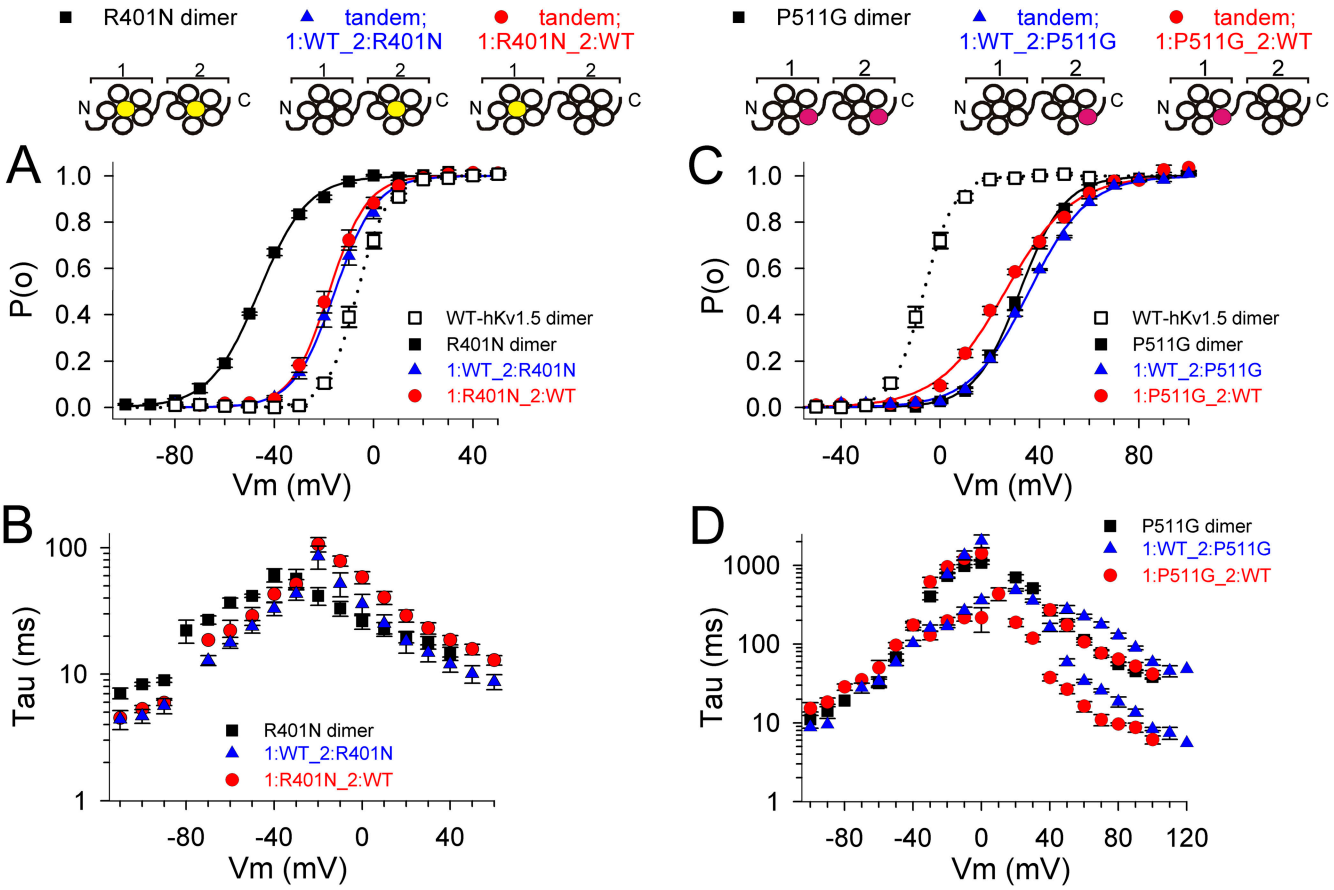

FIGURE 4. Tandem constructs with either R401N or P511G mutant subunits. (A) Voltage dependence of activation of the tandems with a configuration as indicated by the cartoon. In this illustration, the subunit with the R401N mutation is represented by a yellow segment. The activation curves of both tandem configurations 1:WT_2:R401N (blue triangles) and 1:R401N_2:WT (red circles) were similar and clearly shifted toward WT-hKv1.5 dimer values (dotted line), compared with the R401N dimer (black squares). (B) The activation and deactivation time constants of both R401N/WT tandem configurations were similar to those of the R401N dimer. (C) Activation curves of the tandem constructs containing P511G as indicated in the cartoon, with the P511G mutation illustrated with a purple segment. The activation curve of the tandem configuration 1:WT_2:P511G (blue triangles) resembled quite well to the P511G dimer (black squares). The voltage dependence of activation of the tandem with the opposite configuration 1:P511G_2:WT (red circles) was slightly shifted toward negative potentials compared with the P511G dimer; but compared with WT (dotted line), the midpoint was still at positive potentials. (D) Time constants of both P511G/WT tandem configurations were similar to those of the P511G dimer. For raw current traces of dimers and tandem constructs see Fig. S2 (available at http://www.jgp.org/cgi/content/full/jgp.200409194/DC1).

R401N+P511G dimer (both subunits containing both mutations), the condition in which the S4 mutation always compensates the S6 mutation independent of an inter- or intrasubunit interaction. The tandems with either the 1:WT_2:R401N+P511G or the 1:R401N+P511G_2:WT configuration resulted in functional channels with a voltage dependence of activation nearly indistinguishable from the reference R401N+P511G dimer (Fig. 5 A; Table I). The activation and deactivation time constants were best described by a double exponential function (Fig. 5 B) and displayed a marked slowing of deactivation, similar to the reference R401N+P511G dimer. These results clearly indicate that the S4 mutation (R401N) compensated the voltage dependence of activation of the S6 mutation (P511G) when both mutations were located within the same subunit. The raw current traces for all constructs in Fig. 5 are shown in Fig. S3 (available at http://www.jgp.org/cgi/content/full/jgp.200409194/DC1).

To exclude an intersubunit interaction, tandem constructs with both the S4 and the S6 mutation in a separate subunit (Fig. 5 C, top) were used. The channels containing the 1:R401N_2:P511G tandem had a midpoint potential similar to the P511G dimer (Fig. 5 C; Table I), indicating that no compensation of the voltage dependence of activation had occurred. The tandem with the opposite configuration 1:P511G_2:R401N resulted in a channel with an activation curve that was slightly shifted (~8 mV) toward negative potentials compared with the P511G dimer. However, compared with the reference R401N+P511G dimer, it was still

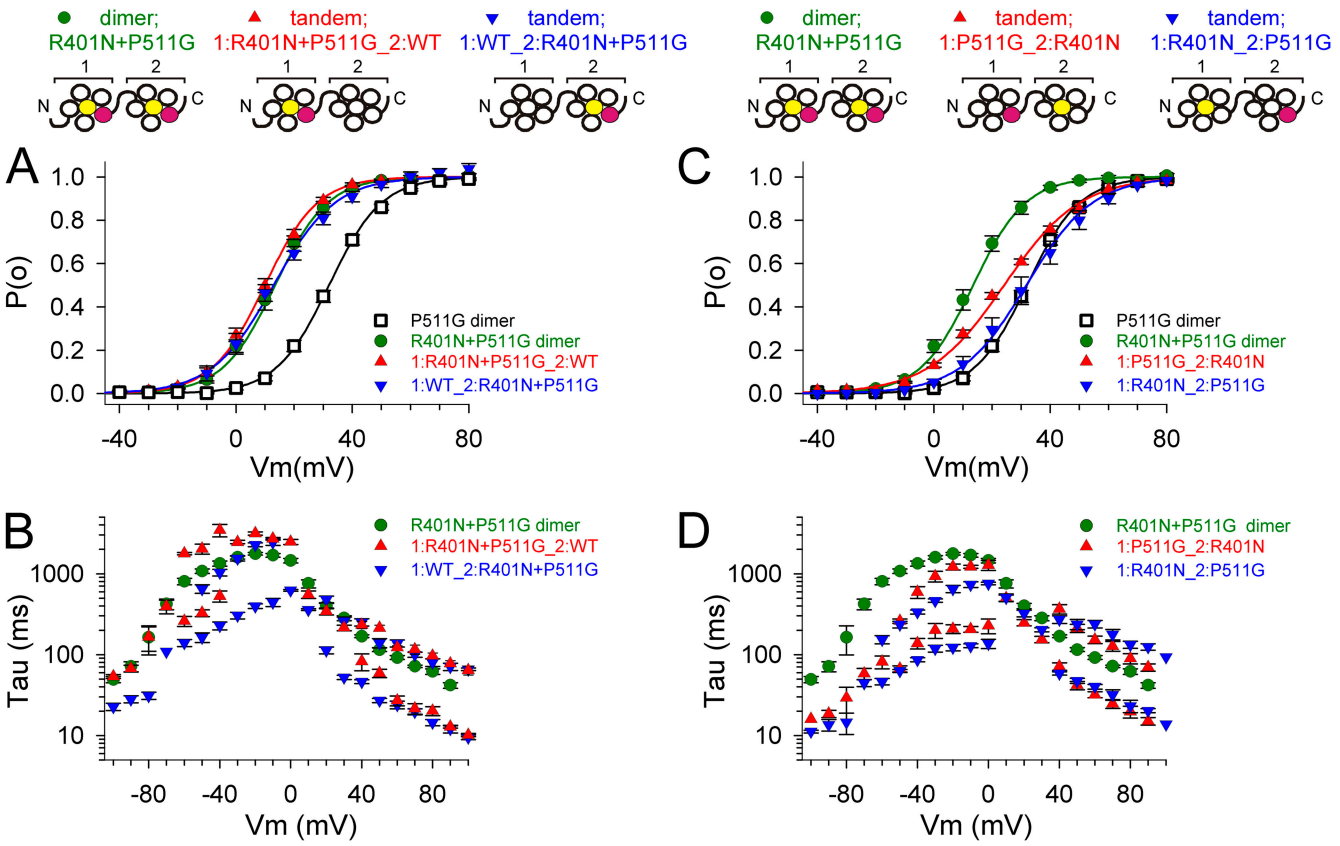

FIGURE 5. Tandems to discriminate between an inter- or intrasubunit interaction. (A) Voltage dependence of activation with tandems containing one WT and one double mutant R401N+P511G subunit, compared with the R401N+P511G dimer. The cartoon depicts the configuration with color coding as in Fig. 4. Both tandem constructs displayed a voltage dependence of activation similar to that of the reference R401N+P511G dimer (green circles). (B) The deactivation time constants of the 1:WT_2:R401N+P511G tandem (blue inverted triangles) were slightly faster and these of the 1:R401N+P511G_2:WT tandem (red triangles) nearly identical to those of the reference R401N+P511G dimer. (C) Voltage dependence of activation of tandems with a single R401N and P511G mutation, each in separate subunits as indicated in the cartoon. These tandem configurations 1:R401N_2:P511G and 1:P511G_2:R401N would demonstrate an intersubunit interaction if present. The tandem 1:R401N_2:P511G (blue inverted triangles) had a midpoint of activation comparable with the P511G dimer (black squares). The tandem with the opposite configuration 1:P511G_2:R401N (red triangles) was slightly shifted toward negative potentials compared with P511G dimer; but compared with the reference R410N+P511G dimer (green circles), the midpoint of activation was still at positive potentials. (D) The deactivation time constants of both 1:R401N_2:P511G and 1:P511G_2:R401N were clearly faster than those of the reference R401N+P511G dimer. For raw current traces of tandem constructs see Fig. S3 (available at http://www.jgp.org/cgi/content/full/jgp.200409194/DC1).

quite positive (Fig. 5 C). The activation and deactivation time constants of both 1:R401N_2:P511G and 1:P511G_2:R401N were also best approximated with a double exponential function. Despite this, both configurations deactivated faster than the reference R401N+P511G dimer, unrelated to the shifted voltage dependence of activation (Fig. 5 D).

DISCUSSION

A voltage-gated K^+ channel operates by sensing the transmembrane voltage (S4 being the main component of the voltage sensor) and subsequently opening a gate (in *Shaker*-type channels, the lower part of S6 contributes to the intracellular gate). Since these channel proteins are tetramers of tightly associated α-subunits, this coupling might occur within the same subunit or between neighboring α-subunits. To address this question, we selected mutations in S4 and S6 that shifted the voltage dependence of activation in the opposite direction. We hypothesized that we could take advantage of the compensation of these shifts when both mutations "communicated" with each other through a coupling mechanism within or between subunits. To exploit this strategy, at least two requirements had to be fulfilled: (1) both mutations should affect gating independently and their shifted voltage dependencies should compensate each other, and (2) the stoichiometry of subunits within a channel should be controlled.

The S4 (R401N) and S6 (P511G) mutation shifted the voltage dependence of activation, compared with WT-hKv1.5, toward negative (Miller and Aldrich, 1996)

and positive potentials, respectively (Fig. 1 and 3; see also Labro et al., 2003). Combining both mutations shifted the activation curve back toward WT (Fig. 1 B). Since both mutations are located in different regions of the channel protein, their compensatory effect on channel gating would therefore not be due to close packing of both residues, and we hypothesize that they communicated through a coupling mechanism. To control the stoichiometry of the mutations within a functional channel, tandem constructs were used (Tytgat and Hess, 1992). Tandems with one mutant (R401N or P511G) and one WT subunit indicated that both subunits of the tandem participated in a functional channel (Fig. 4) (McCormack et al., 1992). Furthermore, a tandem with two "different" subunits displayed, in contrast with homodimeric tandems, two components in the kinetics of current activation. Finally, the comparison of a cotransfection with a tandem construct supported the idea that both subunits of the tandem were integrated in a functional channel.

The use of these mutations in a controlled stoichiometry allowed us to address whether the coupling mechanism originates within or between subunits. The intrasubunit nature of the interaction was supported by the results of the tandems 1:R401N+P511G_2:WT and 1:WT_2:R401N+P511G because (1) the midpoint potential was similar to the reference R401N+P511G dimer and (2) both tandems deactivated extremely slow, a feature typical for the double mutant R401N+P511G and not observed with the tandems 1:R401N_2:P511G and 1:P511G_2:R401N (Fig. 5, B and D). Furthermore, the results for the tandem configurations 1:R401N_2:P511G and 1:P511G_2:R401N do not support an intersubunit interaction since the midpoint was similar to that of the P511G dimer and that of the tandem constructs with a WT subunit instead of the mutant R401N (tandems 1:WT_2:P511G and 1:P511G_2:WT, respectively; Fig. 4 B).

In the gating model based on the 3D crystal structure of the bacterial voltage-gated K^+ channel KvAP, the movement of the voltage sensor "paddle" exerts force on S5, through the S4–S5 linker, pulling S5 away from the central pore axis (Jiang et al., 2003). It was suggested that S5 and S6 move together as one unit, resulting in pore widening. This model is consistent with an intrasubunit interaction, but admittedly, the deduction of a dynamic gating mechanism from a static crystal structure remains inconclusive. Moreover, recent results suggest that the voltage sensor of *Shaker*-type channels differs from that of KvAP (Gandhi et al., 2003; Laine et al., 2003; Lee et al., 2003; Ahern and Horn, 2004; Durell et al., 2004; Shrivastava et al., 2004; Starace and Bezanilla, 2004). An alternative gating hypothesis for eukaryotic K^+ channels is based on the direct coupling of the S4–S5 linker to the COOH-terminal part of S6 (Lu et al., 2002; Tristani-Firouzi et al., 2002; Ding and Horn, 2003; Decher et al., 2004). Although we cannot distinguish between these two gating hypotheses, our results provide functional support for the idea that an important part of the coupling operates within the same subunit.

A recent model positions the S4–S5 linker of one subunit in close proximity to the COOH-terminal S6 part of a neighboring subunit (Laine et al., 2003). This model was based on cysteine interactions between the extracellular ends of S4 and S5 of a neighboring subunit. However no conclusive experimental data was available for inter- or intrasubunit interactions between the S4–S5 linker and S6 at the intracellular face. In recent mathematical models, both intra- and intersubunit interactions are present between the S4–S5 linker and S6 (Durell et al., 2004).

An intrasubunit interaction between voltage sensing and gate opening is also consistent with various kinetic models of channel gating. Within the three-state four-subunit model proposed by Zagotta et al. (1994), ion conduction through the channel pore requires two independent conformational changes in each subunit followed by a final cooperative step. Schoppa et al. extended this scheme with one extra concerted transition and suggested a 3+2' model (Schoppa and Sigworth, 1998). The gating charge measured in *Shaker*(IR) consists of a total between 12 and 13 e_0 per channel (Schoppa et al., 1992; Noceti et al., 1996; Seoh et al., 1996) but only 0.4 to 0.5 e_0 of gating charge is moved during the last concerted transitions (Rodriguez and Bezanilla, 1996; Ledwell and Aldrich, 1999). Thus, in both models, the earlier independent conformational changes (before the final concerted transition) account for most of the gating charge moved. Recently, it was proposed that the Hill coefficient can be used as an estimation for the magnitude of cooperativity in channel gating (Yifrach, 2004). For the *Shaker* K^+ channel, this value was low, which suggested that the gating indeed occurs through many independent transitions.

However, because of the fourfold symmetry, these mathematical models do not definitely discriminate between molecular inter- or intrasubunit interactions. Our results suggest that the independence of the earlier conformational changes in both models reflects an intrasubunit interaction between voltage sensing and gating, at least up to the final step(s). Furthermore, our results indicate that within a heterotetrameric channel, the channel opening is largely determined by the subunit with a gate that activates at the most positive voltages. For example, the voltage dependence of activation of tandems with one WT and one R401N subunit is close to WT values, irrespective of its location as first or second subunit of the tandem (Fig. 4 A). This holds for the P511G/WT tandems in which the voltage depen-

dence is shifted toward P511G values (Fig. 4 C). In contrast, the results obtained with a *Shaker* chimera in which the S4 sequence was substituted by the corresponding *Shaw* sequence (Smith-Maxwell et al., 1998; Ledwell and Aldrich, 1999) could only be explained by subunit cooperativity. In this case, presumably a final concerted transition was altered by substituting the complete S4 segment. In our case, a single point mutation did not appear to influence the concerted transition, but apparently impacted on the independent conformational changes within each subunit. An interaction of S4 with S6 through the S4–S5 linker may represent the molecular substrate for this coupling. Nevertheless, our results do not exclude the existence of subunit cooperativity in the final concerted transition leading to channel opening. In conclusion, we propose that an intrasubunit coupling mechanism between voltage sensing and gate opening operates independently within each α-subunit of the tetramer and underlies the independent conformational changes within each subunit, priming each subunit for the final concerted (cooperative) transition(s).

We want to thank I. Bellens and T. Bruyns for technical assistance in the molecular biology.

A.J. Labro is a fellow with the Vlaams Instituut voor de bevordering van het Wetenschappelijk-Technologisch Onderzoek in de Industrie (IWT). This work was supported by Flanders Institute for Biotechnology grant PRJ05, Interuniversity Attraction Poles program P5/19 of the Belgian Federal Science Policy Office, Fonds voor Wetenschappelijk Onderzoek Vlaanderen grant FWO-G0421102, and National Institutes of Health/National Heart, Lung, and Blood Institute grant HL59689.

David C. Gadsby served as editor.

Submitted: 11 October 2004
Accepted: 6 December 2004

REFERENCES

Ahern, C.A., and R. Horn. 2004. Specificity of charge-carrying residues in the voltage sensor of potassium channels. *J. Gen. Physiol.* 123:205–216.

Bezanilla, F. 2000. The voltage sensor in voltage-dependent ion channels. *Physiol. Rev.* 80:555–592.

Decher, N., J. Chen, and M.C. Sanguinetti. 2004. Voltage-dependent gating of hyperpolarization-activated, cyclic nucleotide-gated pacemaker channels: molecular coupling between the S4-S5 and C-linkers. *J. Biol. Chem.* 279:13859–13865.

del Camino, D., and G. Yellen. 2001. Tight steric closure at the intracellular activation gate of a voltage-gated K^+ channel. *Neuron.* 32:649–656.

Ding, S., and R. Horn. 2003. Effect of S6 tail mutations on charge movement in *Shaker* potassium channels. *Biophys. J.* 84:295–305.

Doyle, D.A., J.M. Cabral, R.A. Pfuetzner, A. Kuo, J.M. Gulbis, S.L. Cohen, B.T. Chait, and R. MacKinnon. 1998. The structure of the potassium channel: molecular basis of K^+ conduction and selectivity. *Science.* 280:69–77.

Durell, S.R., I.H. Shrivastava, and H.R. Guy. 2004. Models of the structure and voltage-gating mechanism of the Shaker K^+ channel. *Biophys. J.* 87:2116–2130.

Gandhi, C.S., E. Clark, E. Loots, A. Pralle, and E.Y. Isacoff. 2003. The orientation and molecular movement of a K^+ channel voltage-sensing domain. *Neuron.* 40:515–525.

Jiang, Y., A. Lee, J. Chen, M. Cadene, B.T. Chait, and R. MacKinnon. 2002. Crystal structure and mechanism of a calcium-gated potassium channel. *Nature.* 417:515–522.

Jiang, Y., A. Lee, J. Chen, V. Ruta, M. Cadene, B.T. Chait, and R. MacKinnon. 2003. X-ray structure of a voltage-dependent K^+ channel. *Nature.* 423:33–41.

Kuo, A., J.M. Gulbis, J.F. Antcliff, T. Rahman, E.D. Lowe, J. Zimmer, J. Cuthbertson, F.M. Ashcroft, T. Ezaki, and D.A. Doyle. 2003. Crystal structure of the potassium channel KirBac1.1 in the closed state. *Science.* 300:1922–1926.

Labro, A.J., A.L. Raes, I. Bellens, N. Ottschytsch, and D.J. Snyders. 2003. Gating of *Shaker*-type channels requires the flexibility of S6 caused by prolines. *J. Biol. Chem.* 278:50724–50731.

Laine, M., M.C. Lin, J.P. Bannister, W.R. Silverman, A.F. Mock, B. Roux, and D.M. Papazian. 2003. Atomic proximity between S4 segment and pore domain in Shaker potassium channels. *Neuron.* 39:467–481.

Ledwell, J.L., and R.W. Aldrich. 1999. Mutations in the S4 region isolate the final voltage-dependent cooperative step in potassium channel activation. *J. Gen. Physiol.* 113:389–414.

Lee, H.C., J.M. Wang, and K.J. Swartz. 2003. Interaction between extracellular Hanatoxin and the resting conformation of the voltage-sensor paddle in Kv channels. *Neuron.* 40:527–536.

Li-Smerin, Y., D.H. Hackos, and K.J. Swartz. 2000. A localized interaction surface for voltage-sensing domains on the pore domain of a K^+ channel. *Neuron.* 25:411–423.

Liman, E.R., J. Tytgat, and P. Hess. 1992. Subunit stoichiometry of a mammalian K^+ channel determined by construction of multimeric cDNAs. *Neuron.* 9:861–871.

Lu, Z., A.M. Klem, and Y. Ramu. 2002. Coupling between voltage sensors and activation gate in voltage-gated K^+ channels. *J. Gen. Physiol.* 120:663–676.

McCormack, K., L. Lin, L.E. Iverson, M.A. Tanouye, and F.J. Sigworth. 1992. Tandem linkage of Shaker K^+ channel subunits does not ensure the stoichiometry of expressed channels. *Biophys. J.* 63:1406–1411.

Miller, A.G., and R.W. Aldrich. 1996. Conversion of a delayed rectifier K^+ channel to a voltage-gated inward rectifier K^+ channel by three amino acid substitutions. *Neuron.* 16:853–858.

Noceti, F., P. Baldelli, X.Y. Wei, N. Qin, L. Toro, L. Birnbaumer, and E. Stefani. 1996. Effective gating charges per channel in voltage-dependent K^+ and Ca^{2+} channels. *J. Gen. Physiol.* 108:143–155.

Rodriguez, B.M., and F. Bezanilla. 1996. Transitions near the open state in *Shaker* K^+-channel - probing with temperature. *Neuropharmacology.* 35:775–785.

Schoppa, N.E., K. McCormack, M.A. Tanouye, and F.J. Sigworth. 1992. The size of the gating charge in wild type and mutant *Shaker* potassium channels. *Science.* 255:1712–1715.

Schoppa, N.E., and F.J. Sigworth. 1998. Activation of Shaker potassium channels. III. An activation gating model for wild-type and V2 mutant channels. *J. Gen. Physiol.* 111:313–342.

Seoh, S.A., D. Sigg, D.M. Papazian, and F. Bezanilla. 1996. Voltage-sensing residues in the S2 and S4 segments of the *Shaker* K^+ channel. *Neuron.* 16:1159–1167.

Shrivastava, I.H., S.R. Durell, and H.R. Guy. 2004. A model of voltage gating developed using the KvAP channel crystal structure. *Biophys. J.* 87:2255–2270.

Smith-Maxwell, C.J., J.L. Ledwell, and R.W. Aldrich. 1998. Role of the S4 in cooperativity of voltage-dependent potassium channel activation. *J. Gen. Physiol.* 111:399–420.

Starace, D.M., and F. Bezanilla. 2004. A proton pore in a potassium channel voltage sensor reveals a focused electric field. *Nature.* 427:548–553.

Tamkun, M.M., K.M. Knoth, J.A. Walbridge, H. Kroemer, D.M. Roden, and D.M. Glover. 1991. Molecular cloning and characterization of two voltage-gated K^+ channel cDNAs from human ventricle. *FASEB J.* 5:331–337.

Tristani-Firouzi, M., J. Chen, and M.C. Sanguinetti. 2002. Interactions between S4-S5 linker and S6 transmembrane domain modulate gating of HERG K^+ channels. *J. Biol. Chem.* 277:18994–19000.

Tytgat, J., and P. Hess. 1992. Evidence for cooperative interactions in potassium channel gating. *Nature.* 359:420–423.

Yifrach, O. 2004. Hill coefficient for estimating the magnitude of cooperativity in gating transitions of voltage-dependent ion channels. *Biophys. J.* 87:822–830.

Zagotta, W.N., T. Hoshi, and R.W. Aldrich. 1994. *Shaker* potassium channel gating. III: Evaluation of kinetic models for activation. *J. Gen. Physiol.* 103:321–362.